Article

Discovery Medicine 2026; 38(204): 118–131
https://doi.org/10.24976/Discov.Med.202638204.10

Human Umbilical Cord Mesenchymal Stem Cell-Derived Exosomes Promote Morphological and Functional Repair of Uterine Scar Defects After Caesarean Section

Juan Jin[1], Qian Pu[2], Yaxin Hu[3], Shuixiu Yang[4], Dajiang Lu[5], Lei Yu[2,*], Liping Chen[6,*]

[1]Department of Obstetrics, The People's Hospital of Qiannan, 558000 Duyun, Guizhou, China
[2]Central Laboratory, Guiyang Maternal and Child Health Care Hospital, 550000 Guiyang, Guizhou, China
[3]Prenatal Diagnosis Center, Affiliated Hospital of Guizhou Medical University, 550000 Guiyang, Guizhou, China
[4]Blood Purification Center, Guiyang Public Health Clinical Center, 550000 Guiyang, Guizhou, China
[5]Department of Gynecology, The People's Hospital of Qiannan, 558000 Duyun, Guizhou, China
[6]Reproductive Medicine Center, Guangdong Armed Police Corps Hospital, 510000 Guangzhou, Guangdong, China
*Correspondence: myyl2004@163.com (Lei Yu); chenlphch@2925.com (Liping Chen)
Submitted: 17 October 2025 Revised: 24 November 2025 Accepted: 11 December 2025 Published: 20 January 2026

Background: A previous caesarean scar defect (PCSD), also referred to as a caesarean scar diverticulum, is a highly prevalent condition, resulting in infertility and uterine rupture. Currently, there are no effective treatment options for treating this condition. Evidence indicates that mesenchymal stem cells (MSCs) promote tissue repair and regeneration. Furthermore, studies have demonstrated that the therapeutic effects of MSCs are mediated by exosomes produced through a paracrine mechanism. Therefore, this study aims to explore the potential of human umbilical cord mesenchymal stem cell-derived exosomes (hUCMSC-Exos) in repairing post-caesarean uterine scar defects in rat models.

Methods: A rat model of PCSD was established using the combination of mechanical injury and infection. Two weeks post-surgery, hUCMSC-Exos were transplanted into the uterine scar area. At 8 weeks post-transplantation, endometrial thickness, myometrial thickness, and fibrosis were assessed using H&E and Masson's trichrome staining. Immunohistochemistry (IHC) and Western blot analysis were performed to evaluate α-smooth muscle actin (α-SMA), transforming growth factor-β1 (TGF-β1), and vascular endothelial growth factor (VEGF) protein levels. The remaining female rats were mated with males, and fertility was examined by euthanizing them at 19 days post-conception.

Results: Excessive collagen deposition and thinning of the endometrium and myometrium were observed in PCSD model rats. Following hUCMSC-Exos transplantation, collagen deposition in the uterine scar decreased ($p < 0.001$), while endometrium thickness, myometrium thickness, and angiogenesis levels all significantly increased ($p < 0.001$). Furthermore, TGF-β1 levels decreased ($p < 0.01$), while α-SMA and VEGF levels increased ($p < 0.001$) after hUCMSC-Exos treatment. Additionally, pregnancy rates improved, and the number of implanted fetuses within the scar area increased ($p < 0.01$).

Conclusion: hUCMSC-Exos exerts significant therapeutic effects by improving both the morphology and function in a previous caesarean scar defect model. hUCMSC-Exos offers a novel, cell-free therapeutic option for patients with PCSD.

Keywords: human umbilical cord mesenchymal stem cells; exosomes; previous caesarean scar defect; uterine scar repair; fertility

Introduction

A Previous caesarean scar defect (PCSD) refers to a condition in which poor healing of the uterine incision leads to thinning of the myometrial layer at the scar site, forming a depression or cavity that communicates with the uterine cavity. Clinically, some patients experience abnormal vaginal bleeding, dysmenorrhea, and chronic pelvic pain [1,2]. Histopathologically, PCSD is characterized by significantly reduced myometrial thickness and replacement of normal uterine smooth muscle by fibrotic tissue at the scar site [3]. PCSD can contribute to infertility and is associated with obstetric complications in subsequent pregnancies, including caesarean scar pregnancy, uterine rupture, pernicious placenta previa, and postpartum hemorrhage [4,5]. As a major long-term complication of caesarean section, its incidence ranges from 19.4% to 88.0% [6]. The etiology is multifactorial and generally involves improper suturing of the uterine incision, postoperative infection, and multiple caesarean sections [7–9].

Currently, there is no universally accepted optimal management for PSCD. Treatment primarily relies on hormonal therapy and surgical intervention. Hormonal therapy can alleviate abnormal vaginal bleeding but does not promote healing, and the symptoms often recur after discontinuation [10,11]. For patients with severe conditions, particularly those with infertility, surgical intervention may be the only effective option, including hysteroscopic, laparo-

scopic, and transvaginal repair approaches [12,13]. However, surgical interventions themselves may induce uterine trauma, and there remains a risk of poor wound healing and the formation of new defects after repair. Therefore, identifying a minimally invasive and highly efficient treatment approach for PCSD is of great clinical significance.

Mesenchymal stem cells (MSCs) are widely recognized for their strong therapeutic potential in regenerative medicine. Among various MSC sources, umbilical cord-derived mesenchymal stem cells (UC-MSCs) have attracted attention due to their ready availability, high proliferative capability, and relatively lower risk of viral infection contamination [14,15]. In a rat model of full-thickness uterine injury, UC-MSCs have been found to promote collagen degradation and angiogenesis, thereby facilitating regeneration of the damaged uterine wall in a uterine scar model [16]. However, stem cell-based therapies also face significant challenges, including limited post-transplantation cell survival, genetic mutations that may induce tumorigenesis or teratogenicity, the risk of vascular embolism from transplanted cells, and limitations related to long-term storage and transportation, all of which hinder the broader clinical application of MSC-based treatment [17].

In recent years, increasing evidence has demonstrated that the therapeutic effects of stem cells are primarily mediated by exosomes—extracellular vesicles secreted via paracrine mechanisms. These vesicles contain proteins, lipids, DNA, mRNA, non-coding RNAs, and other bioactive molecules that facilitate signal transduction between cells and modulate diverse biological processes [18–21]. Previous studies have revealed that exosomes are widely used in regenerative medicine and have reported favorable outcomes in treating various diseases, including kidney injury [22], lung injury [23], spinal cord injury [24], premature ovarian insufficiency [25], and intrauterine adhesions [26]. Therefore, exosome-based tissue approaches for tissue regeneration are being extensively investigated as a promising therapeutic option.

Although the regenerative potential of exosomes derived from umbilical cord mesenchymal stem cells (UCMSC-Exos) has been demonstrated in numerous animal models, studies specifically assessing their role in uterine scar repair remain limited. A study by Zeng *et al*. [27] validated the efficacy of hUCMSC-Exos in repairing uterine scar defects in rats; however, their model was developed in non-pregnant rats, which do not adequately represent caesarean section-related uterine scar defects. Therefore, we established a rat model of post-caesarean section uterine scar defect induced by a combination of infection and physical injury. Using this model, we conducted a comparative assessment of hUCMSCs and hUCMSC-Exos to explore the effects of hUCMSC-Exos transplantation on uterine morphology and fertility outcomes in rats with PCSD.

Materials and Methods

Culture of hUCMSCs

Primary hUCMSCs were purchased from Zhong Qiao Xin Zhou Biotechnology Co., Ltd. (sourced from the National Stem Cell Transformation Resource Bank, ZB09BA, Shanghai, China). The certificate of analysis indicates that these cells are positive for the mesenchymal-specific markers CD73, CD90, and CD105, and negative for CD11, CD19, CD31, CD34, CD45, and HLA-DR. Microbiological testing, such as mycoplasma identification, was negative. Furthermore, the cells differentiated into adipocytes, osteoblasts, and chondrocytes under appropriate *in vitro* induction conditions.

After thawing, primary hUCMSCs were resuspended in DMEM/F12 basal medium (C11330500BT, Gibco, USA) containing 10% FBS (04-001-1A, BioInd, Israel) and 1% penicillin-streptomycin dual antibiotic (03-031-1B, BioInd, Israel). Cells were seeded in 75 cm^2 flasks at a density of 1×10^7 cells/mL and maintained in an incubator at 37 °C with 5% CO_2 (MCO-18AIC, SANYO, Japan). After 48 hours, the medium was replaced based on cell attachment, and then the medium was refreshed every 2 days to remove non-adherent cells. Simultaneously, cell morphology and growth were monitored using an inverted microscope (CKX31, Olympus, Japan). When cultures reached approximately 90% confluence, cells were passaged at a 1:3 ratio. hUCMSCs at passages 5–8 were used for subsequent experiments.

Isolation and Characterization of hUCMSC-Exosomes

When hUCMSCs at passages 5–8 reached about 90% confluence, the cells were rinsed with PBS, and the culture medium was replaced with serum-free DMEM/F12. After 48 hours of serum-free culture, the conditioned medium was collected for exosome extraction. After filtration (0.22 μm, Millipore, USA), the supernatant was centrifuged (Sorvall WXULTRA, Thermo Fisher Scientific, USA) at 4 °C and 120,000 ×g for 2 hours. The resulting hUCMSC-Exos pellet was resuspended in PBS and stored at –80 °C until use. The morphology and size of the exosomes were observed under a transmission electron microscope (TEM, HITACHI H-7000FA, Hitachi, Japan). Exosome protein content, used as an indicator of exosome concentration, was quantified using the BCA protein assay kit (P0010, Beyotime Biotechnology, Shanghai, China).

Briefly, the BSA standard was prepared by serial dilution and dispensed into designated wells of a 96-well plate. Subsequently, a 10-fold dilution of the exosome suspension was then added to new wells. The BCA working solution was prepared by mixing Solutions A and B at a 50:1 volume ratio, and 0.2 mL of the mixture was added to each well. The culture plate was sealed with a membrane and incubated at 37 °C for 30 minutes. Absorbance at 562 nm

(OD562) was measured using a microplate reader (Multiskan MK3, Thermo Fisher, USA). Furthermore, a standard curve was generated by linear regression of standard protein concentration against OD values, and this equation was used to determine the protein concentration of the exosomes. To confirm exosome identity, Western blot analysis was performed to detect the expression of CD63 (AF5117, Affinity, USA) and CD81 (DF2306, Affinity, USA) in exosomes.

Establishment of the Animal PCSD Model and Grouping

Animal experiments were approved by the Animal Care Welfare Committee of Guizhou Medical University (Approval number: 2304384). Sprague-Dawley (SD) rats were purchased from Zhejiang Vital River Laboratory Animal Technology Co., Ltd. (License No.: SCXK(Zhe)2019-0001, Pinghu, China). Virgin female rats were 8–9 weeks old, weighing 220 ± 20 g, and male rats were 9–10 weeks old, weighing 280 ± 20 g. All rats were housed under SPF conditions and acclimatized for one week before experimentation.

Vaginal smears were performed daily between 9:00 and 10:00 AM to observe estrous cycles based on changes in vaginal epithelial cells. Female rats with four consecutive regular estrous cycles were selected for mating experiments. Females and males were housed together at a 2:1 ratio. The presence of sperm in the vaginal smear the next morning was designated as gestational day 0. Fifty-eight pregnant rats, corresponding to 116 uterine horns, were randomly divided into 3 groups: normal delivery group (8 rats, Normal group, n = 16 uterine horns), standard caesarean section group (10 rats, Caesarean group, n = 20 uterine horns), and PCSD model group (40 rats, n = 80 uterine horns).

A preliminary experiment confirmed the development of the PCSD model with a success rate of 85%. Except for the normal group, which delivered naturally/vaginally, all pregnant rats in other groups underwent caesarean section on gestational day 19. Rats were anesthetized by intraperitoneal injection of 3% sodium pentobarbital (50 mg/kg, P3761, Haoran Bio, Shanghai, China). A midline abdominal incision was made to expose the uterine horns.

In the caesarean group, an 8-cm longitudinal incision was made on the antimesenteric side of each uterine horn, 2 cm above the cervical bifurcation. Fetuses and placentas were removed, and the incision ends were marked using No. 1 silk sutures. The uterine incision was closed with continuous 4-0 absorbable sutures, and the abdominal incision was closed in layers.

In the PCSD model group, lipopolysaccharide (LPS; 0.5 mg/mL, 1 mL/kg, L8880-10mg, Solarbio, Beijing, China) was injected at multiple points into the myometrium on both sides of the uterine incision. Simultaneously, both sides of the incision were treated with electrocoagulation using an electrofrequency ion therapy apparatus (power 10 W, Likang Electronic Medical Equipment Co., Ltd., Guilin, China). The remaining surgical procedures were similar to those in the caesarean group. Furthermore, penicillin (80,000 IU/100 g, H13021634, Zhongnuo Pharmaceutical, Shijiazhuang, China) was administered intraperitoneally during surgery and again on the first postoperative day. No rats died in the caesarean group. In the PCSD model group, five rats died within 48 hours, likely due to LPS-induced sepsis. However, five surviving rats were randomly excluded, leaving 30 rats for subsequent experiments. These rats were randomly divided into three groups: model group (10 rats, n = 20 uterine horns), hUCMSCs treatment group (MSCs group, 10 rats, n = 20 uterine horns), and hUCMSC-Exos treatment group (MSC-Exos group, 10 rats, n = 20 uterine horns).

Two weeks after model development, the rats were re-anesthetized and underwent repeat laparotomy. Using a 1-mL syringe, multiple intramural injections were administered from top to bottom within the previously marked area of the uterine horn. In the caesarean and model groups, each uterine horn was injected with 0.2 mL PBS. In the MSCs group, each uterine horn received 0.2 mL hUCMSCs suspension (containing 5×10^6 cells/mL). In the MSC-Exos group, each uterine horn was injected with 0.2 mL hUCMSC-Exos suspension (exosome protein concentration adjusted to 50 µg/0.2 mL). However, the normal group received no such intervention.

Eight weeks after treatment, 4 rats from the normal group and 5 rats from each surgical group were euthanized by intraperitoneal injection of 3% sodium pentobarbital (150 mg/kg). Bilateral uterine horn tissues were collected (entire uterine length in the normal group and only the scar segment in the other groups) for subsequent experiments. The collected tissues were divided into 2 parts. One portion was processed into paraffin sections for histopathological observation and immunohistochemical assessment of protein localization, and the other portion was used for total protein extraction and Western blot analysis.

Histological Analysis

One uterine horn from each group was fixed in 4% paraformaldehyde (DF0135, Leagene Biotechnology, Beijing, China), embedded in paraffin, and sectioned into 4-um-thick paraffin slices, ensuring that each section contained a complete transverse uterine cross-section. Sections were stained with H&E and Masson staining following standard protocols. Endometrial thickness, myometrial thickness at the scar site, and the percentage area of collagen fibers were determined using Image-Pro Plus 6.0 software (IPP 6.0). Morphological changes were observed under a light microscope (CX31-12C04, Olympus, Japan). For H&E-stained sections, three perpendicular measurements of endometrial and myometrial thickness (µm) were obtained and then averaged. For the Masson-stained section,

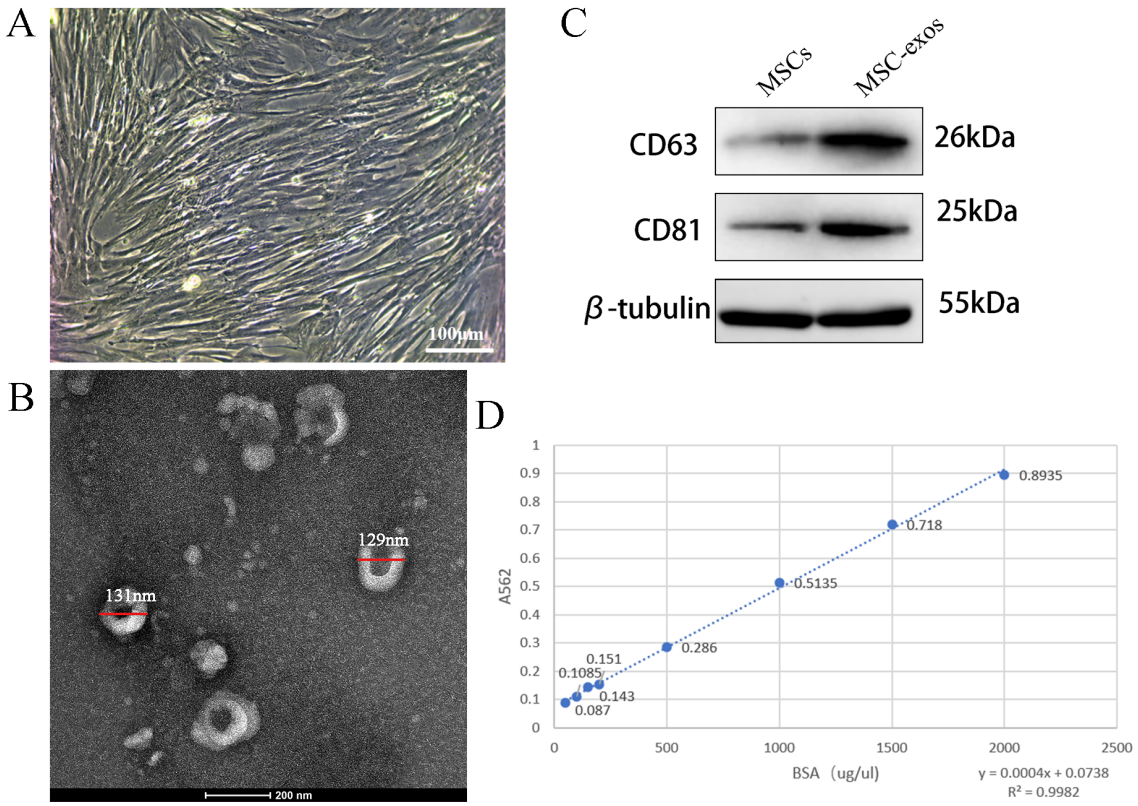

Fig. 1. Identification of hUCMSC-Exos. (A) Morphology of 5th generation hUCMSCs cultured for 5 days (magnification: 100×). (B) Transmission electron microscopy of hUCMSCs-Exos. (C) Western blot analysis to detect the expression of hUCMSC-Exos specific markers CD63 and CD81. (D) BCA reagent method to measure the protein concentration of hUCMSC-Exos. hUCMSC-Exos, human umbilical cord mesenchymal stem cell-derived exosomes; BCA, bicinchoninic acid.

the ratio of collagen fiber area relative to the total uterine area (excluding the lumen) was calculated using IPP 6.0.

For immunohistochemistry (IHC), tissue sections were incubated with the following primary antibodies (Abcam, UK): anti-α-SMA (α-SMA, 1:2000, ab124964), anti-TGF-β1 (TGF-β1, 1:600, ab215715), and anti-VEGF (VEGF, 1:300, ab32152). Quantitative analysis was conducted using IPP 6.0. For α-SMA, the proportion of positively stained areas in the myometrial scar region relative to the total myometrial area was calculated. For TGF-β1, the number of positive cells in three randomly selected high-power fields within the scar area was counted, and the average optical density was calculated. For VEGF, microvessel density was determined by counting the number of microvessels in three random high-power fields within the scar area and calculating the average. In the normal group, three random uterine regions were selected for comparative analysis, and the average was used as the control.

Western Blot Analysis

Proteins were extracted from the opposite uterine horns of each group, and their concentrations were determined using the BCA assay. Equal amounts of protein (30 μg) were separated by SDS-PAGE and subsequently transferred onto PVDF membranes (0.45 μm, Millipore, USA). Membranes were blocked with TBST containing 5% non-fat milk for one hour to prevent nonspecific binding, then incubated overnight at 4 °C with the following primary antibodies (Abcam, UK): rabbit anti-α-SMA (α-SMA, 1:4000, ab124964), rabbit anti-TGF-β1 (TGF-β1, 1:2000, ab215715), rabbit anti-VEGF (VEGF, 1:3000, ab32152), and rabbit anti-β-Actin (β-Actin, 1:2000, ab8227). The next day, membranes were incubated with HRP-goat anti-rabbit secondary antibody (1:6000, ab6721, Abcam, UK) at room temperature for 1 hour, followed by ECL chemiluminescence detection (P10100, Xinsaimai Bio, Suzhou, China). Band intensities were quantified using ImageJ software, and relative protein expression levels were determined. Each group was analyzed three times, and their average was calculated.

Fertility Assessment

Uterine functional recovery after caesarean section with poor incisional scar healing was assessed by examining the capability to conceive and maintain pregnancy to full-term gestation. Eight weeks post-treatment, the remaining female rats (4 in the normal group, 5 in each of the other four groups) were housed with male rats at a 1:1 ratio.

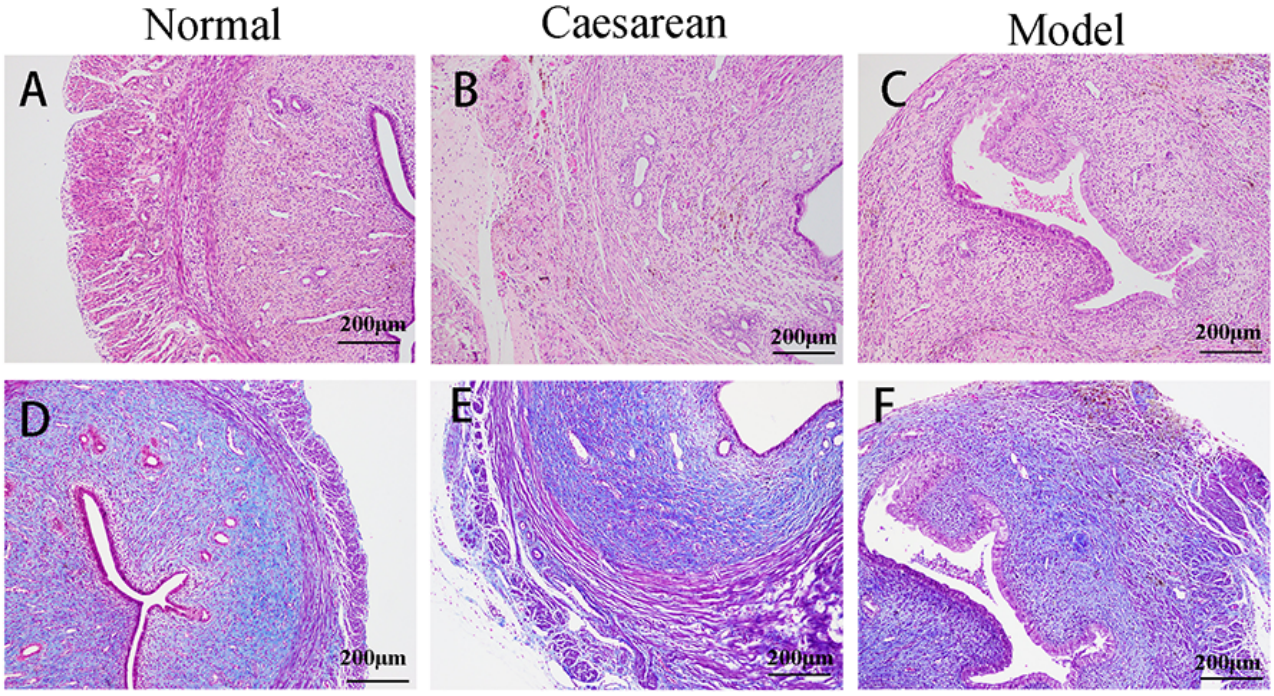

Fig. 2. Establishment of rat model of PCSD. (A–C) H&E staining and (D–F) Masson trichrome staining of uterus in the normal, caesarean, and model groups 2 weeks after dual mechanical + infection injury. Scale bars = 200 μm. PCSD, previous caesarean scar defect; H&E, hematoxylin and eosin staining.

Vaginal smears were collected each morning during mating, and the day on which sperm were first detected was recognized as gestational day 0. On gestational day 19, the rats were euthanized, and both uterine horns were removed to examine the number, size, and viability of fetuses, as well as the site of embryo implantation.

Statistical Analysis

Statistical analysis was conducted using GraphPad Prism (Version 8.4, Inc., La Jolla, CA, USA) and SPSS Statistics Package for Social Science (Version 25.0 IBM Corp., Armonk, NY, USA). Continuous variables were expressed as mean ± standard deviation, and categorical variables as numbers or percentages. For normally distributed variables, comparisons among multiple groups were performed using one-way analysis of variance (ANOVA) and pairwise comparisons were performed using the least significant difference (LSD) tests. Categorical variables (e.g., pregnancy rate) were compared using the χ^2 or Fisher's exact test, as appropriate. A p-value < 0.05 was considered statistically significant.

Results

Characterization of hUCMSC-Exosomes

hUCMSCs exhibited a long spindle shape, adherent growth pattern with uniform, well-defined, plump morphology (Fig. 1A). TEM analysis of hUCMSC-Exos revealed typical cup-shaped vesicles with a diameter of about 30–160 nm (Fig. 1B). Western blot analysis detected the presence of CD63 and CD81 in both hUCMSCs and isolated hUCMSC-Exos, with higher abundance in the exosomes (Fig. 1C). The exosome concentration determined by BCA assay was 1.059 μg/μL (Fig. 1D). These results demonstrate that exosomes were successfully isolated from the conditioned medium of hUCMSCs.

Validation of the Rat PCSD Model Establishment

Two weeks after injury, H&E and Masson staining showed that, compared to the normal group (Fig. 2A,D), the caesarean group demonstrated disorganized endometrial glandular epithelium, poorly defined myometrial layers, mild inflammatory cell infiltration, and an increased area of blue-stained collagen fiber with more intense staining (Fig. 2B,E), indicating scar formation. The model group exhibited significantly thinner endometrium and myometrium, extensive inflammatory cell infiltration, stromal hyperplasia and edema, disrupted or absent smooth muscle fibers, and more pronounced, disorganized collagen deposition (Fig. 2C,F), indicative of a uterine scar defect.

hUCMSC-Exos Transplantation Promotes Restoration of Gross Morphology in Injured Uterine Horns

Rats possess a bicornuate Y-shaped uterus. In the normal group, the uterine horns appeared smooth, rosy, and

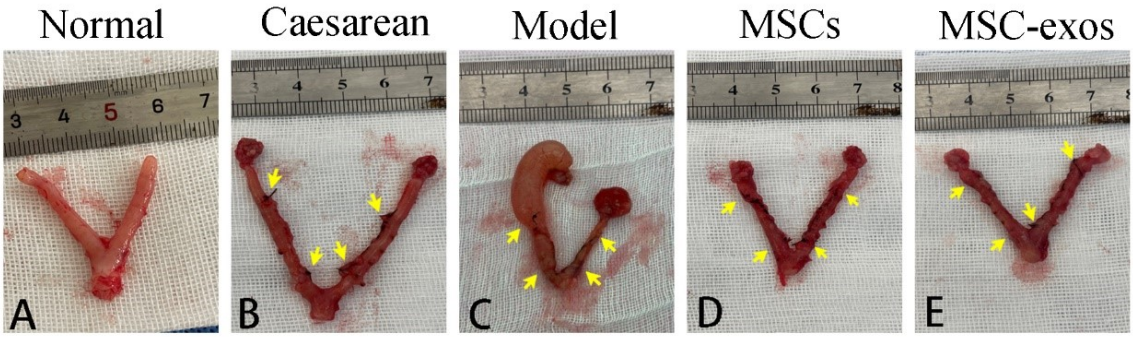

Fig. 3. Morphological observation of the uterine horns in each group at 8 weeks after treatment with different methods. Overall view of both uterine horns: (A) the normal group, (B) the caesarean group, (C) the model group, (D) the MSCs group, and (E) the MSC-Exos group. The scar area is indicated between the two yellow arrows. MSCs, mesenchymal stem cells.

elastic. All surgically treated groups had varying degrees of uterine adhesion, which were more pronounced in the model group, with some animals also developing hydrosalpinx secondary to tubal obstruction. The uterine horns in the caesarean group were larger than in the normal group. Conversely, the MSCs and MSC-Exos groups showed uterine walls with a reddish appearance, uniform thickness, and a texture closely resembling that of normal uteri (Fig. 3).

hUCMSC-Exos Transplantation Promotes Restoration of Tissue Structure in Injured Uterine Horns

H&E staining was used to assess endometrial and myometrial regeneration after hUCMSC-Exos transplantation. At 8 weeks post-transplantation, the MSC-Exos group exhibited the highest endometrial thickness (473.37 $\pm$ 23.85 µm) and myometrial thickness (311.53 $\pm$ 23.75 µm) among all operated groups, significantly greater than the model group ($p < 0.001$), lower than the normal group ($p < 0.05$), and comparable to or slightly greater than the caesarean group. However, there was no statistically significant difference between the MSC-Exos and MSCs groups ($p > 0.05$) (Fig. 4A–E,K,L). These results indicate that both hUCMSCs and hUCMSC-Exos treatments significantly increased endometrial and myometrial thickness of the injured uterine horns.

Masson staining was used to assess fibrosis. In the MSCs (Fig. 4I) and MSC-Exos (Fig. 4J) groups, collagen fibers were significantly reduced, and the fibrotic area was considerably smaller than in the model group (Fig. 4H) (21.00 $\pm$ 2.70% vs 34.18 $\pm$ 2.93%, $p < 0.001$; 18.31 $\pm$ 1.91% vs 34.18 $\pm$ 2.93%, $p < 0.001$, respectively). There were no substantial differences among the caesarean (Fig. 4G), MSCs, and MSC-Exos groups ($p > 0.05$), although all three groups showed higher fibrosis than the normal group (Fig. 4F) ($p < 0.05$). These results indicate that both hUCMSCs and hUCMSC-Exos treatments significantly reduce collagen fiber deposition in the injured uterine horns (Fig. 4M).

hUCMSC-Exos Transplantation Reduces Fibrosis and Promotes Smooth Muscle and Blood Vessel Regeneration in Injured Uterine Horns

IHC of α-SMA was used to evaluate smooth muscle regeneration (Fig. 5A–E,a–e,P). α-SMA expression was predominantly localized to the cytoplasm and nuclei of smooth muscle cells. In the normal group, the myometrium contained abundant brown-yellow granules, whereas only minimal α-SMA staining was observed within the scar region of the model group.

At post-transplantation week-8, the percentage of α-SMA-positive area was significantly higher in MSCs and MSC-Exos groups compared to the model group (20.67 $\pm$ 1.72% vs 12.00 $\pm$ 0.85%, $p < 0.001$; 21.01 $\pm$ 1.72% vs 12.00 $\pm$ 0.85%, $p < 0.001$, respectively). Among the operated groups, the caesarean group had the highest α-SMA-positive area (22.38 $\pm$ 1.17%), although the differences compared with the MSCs and MSC-Exos groups were not statistically significant ($p > 0.05$). These observations showed significantly reduced muscle density in the model group.

IHC of TGF-β1 was used to assess fibrosis (Fig. 5F–J,f–j,Q). TGF-β1 expression was localized to the cytoplasm of endometrial cells and smooth muscle cells. In the normal group, only fewer brown-yellow granules were found in the uterine tissue, whereas the scar region in the model group showed abundant granular staining. At 8 weeks after transplantation, TGF-β1 expression was substantially lower in the MSCs and MSC-Exos groups than in the model group (11.36 $\pm$ 1.40% vs 15.90 $\pm$ 1.92%, $p < 0.05$; 10.77 $\pm$ 1.90% vs 15.90 $\pm$ 1.92%, $p < 0.01$, respectively). Among the operated groups, the caesarean group had the lowest TGF-β1 density (9.55 $\pm$ 0.78%), although the differences relative to the MSCs and MSC-Exos groups were not statistically significant ($p > 0.05$).

IHC of VEGF was used to examine capillary regeneration (Fig. 5K–O,k–o,R). VEGF was localized to the cytoplasm of vascular endothelial cells and served as a clas-

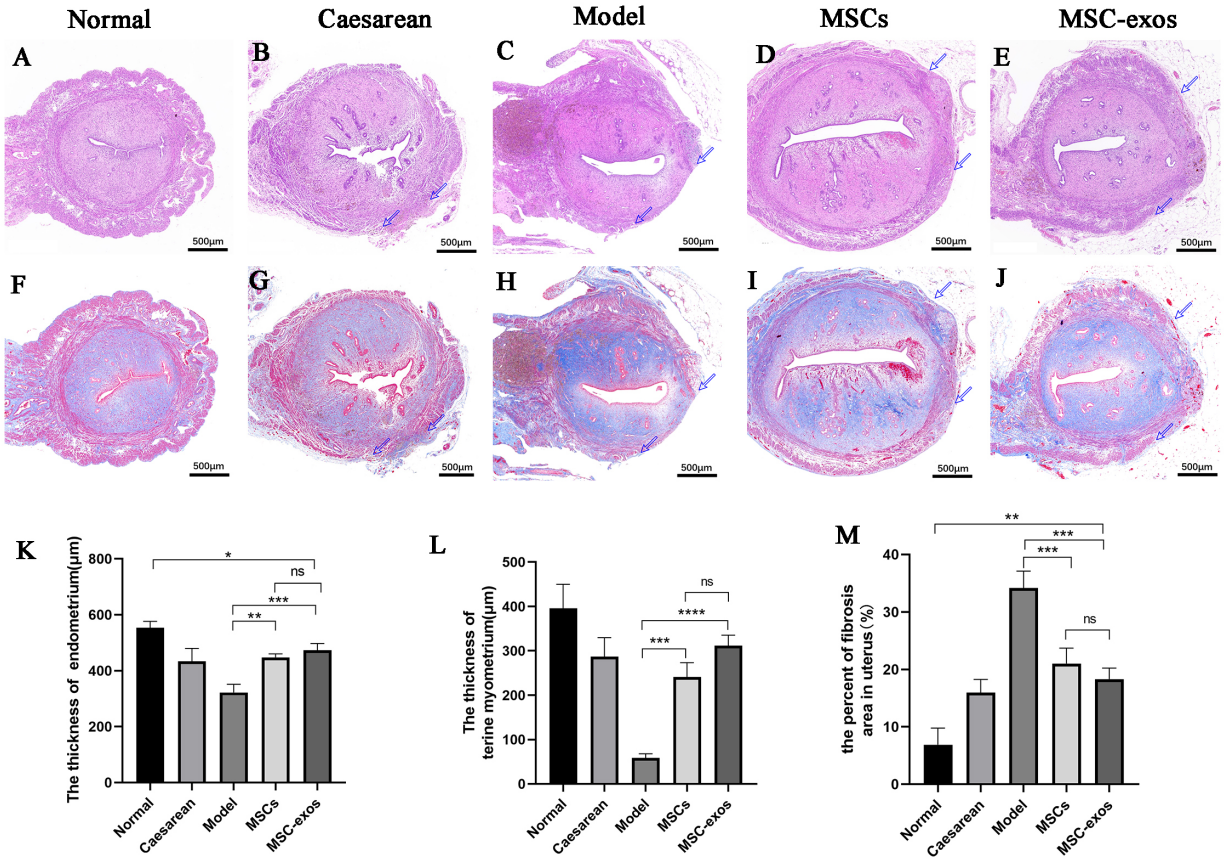

Fig. 4. Endometrial and myometrial regeneration and defibrillation status at 8 weeks post-treatment. (A–E) H&E staining assessed endometrial and myometrial thickness. (F–J) Masson trichrome staining evaluated uterine fibrosis. Scale bar = 500 μm. (K) Statistical analysis of endometrial thickness. (L) Statistical analysis of myometrial thickness. (M) Statistical analysis of the percentage of fibrotic areas in the uterus. *$p < 0.05$, **$p < 0.01$, ***$p < 0.001$, ****$p < 0.0001$, ns $p > 0.05$.

sic microvascular marker. In the normal group, blood vessels were clearly distributed within the uterine wall, with abundant brown-yellow granules in the cytoplasm. In contrast, VEGF expression was significantly reduced in the model group, indicating vascular structure damage. At 8 weeks after transplantation, VEGF expression was highest in the MSC-Exos group, significantly higher than the model group (11.86 ± 1.60 vs 5.43 ± 1.26, $p < 0.0001$) and also higher than in the caesarean group (11.86 ± 1.60 vs 9.04 ± 0.20, $p < 0.05$). However, there was no statistically significant difference among the MSC-Exos, the MSCs, and normal groups ($p > 0.05$).

Western blot analysis was conducted to assess the protein levels of α-SMA, TGF-β1, and VEGF (Fig. 6A). At 8 weeks after transplantation, α-SMA expression in the MSC-Exos group was the highest among all surgical groups and was significantly higher than in the model group (0.90 ± 0.04 vs 0.57 ± 0.03, $p < 0.0001$), but remained lower than in the normal group (0.90 ± 0.04 vs 1.03 ± 0.04, $p < 0.05$). There was no statistically significant difference among the caesarean (0.89 ± 0.04), MSCs (0.86 ± 0.02), and MSC-Exos groups ($p > 0.05$, Fig. 6B).

TGF-β1 protein expression was lowest in the MSC-Exos group among all the operated groups, being significantly lower compared with the model group (0.62 ± 0.04 vs 0.95 ± 0.03, $p < 0.0001$) and also lower than in the caesarean and MSCs groups (0.62 ± 0.04 vs 0.78 ± 0.02, $p < 0.01$; 0.62 ± 0.04 vs 0.79 ± 0.02, $p < 0.01$, respectively). The difference between the MSC-Exos and normal groups (0.54 ± 0.02) was not statistically significant ($p > 0.05$) (Fig. 6C).

VEGF protein expression was significantly higher in both the MSCs and MSC-Exos groups compared with the model group (0.54 ± 0.16 vs 0.11 ± 0.06, $p < 0.01$; 0.66 ± 0.17 vs 0.11 ± 0.06, $p < 0.001$, respectively). However, the difference between the MSCs and MSC-Exos groups was not statistically significant ($p > 0.05$). Among the operated groups, the caesarean group exhibited the highest VEGF expression, though the difference with the MSC-Exos group was not significant (0.82 ± 0.05 vs 0.66 ± 0.17, $p > 0.05$) (Fig. 6D).

These findings indicate that both hUCMSC and hUCMSC-exosome therapies reduce fibrosis in damaged uterine horns by downregulating TGF-β1 and upregulating

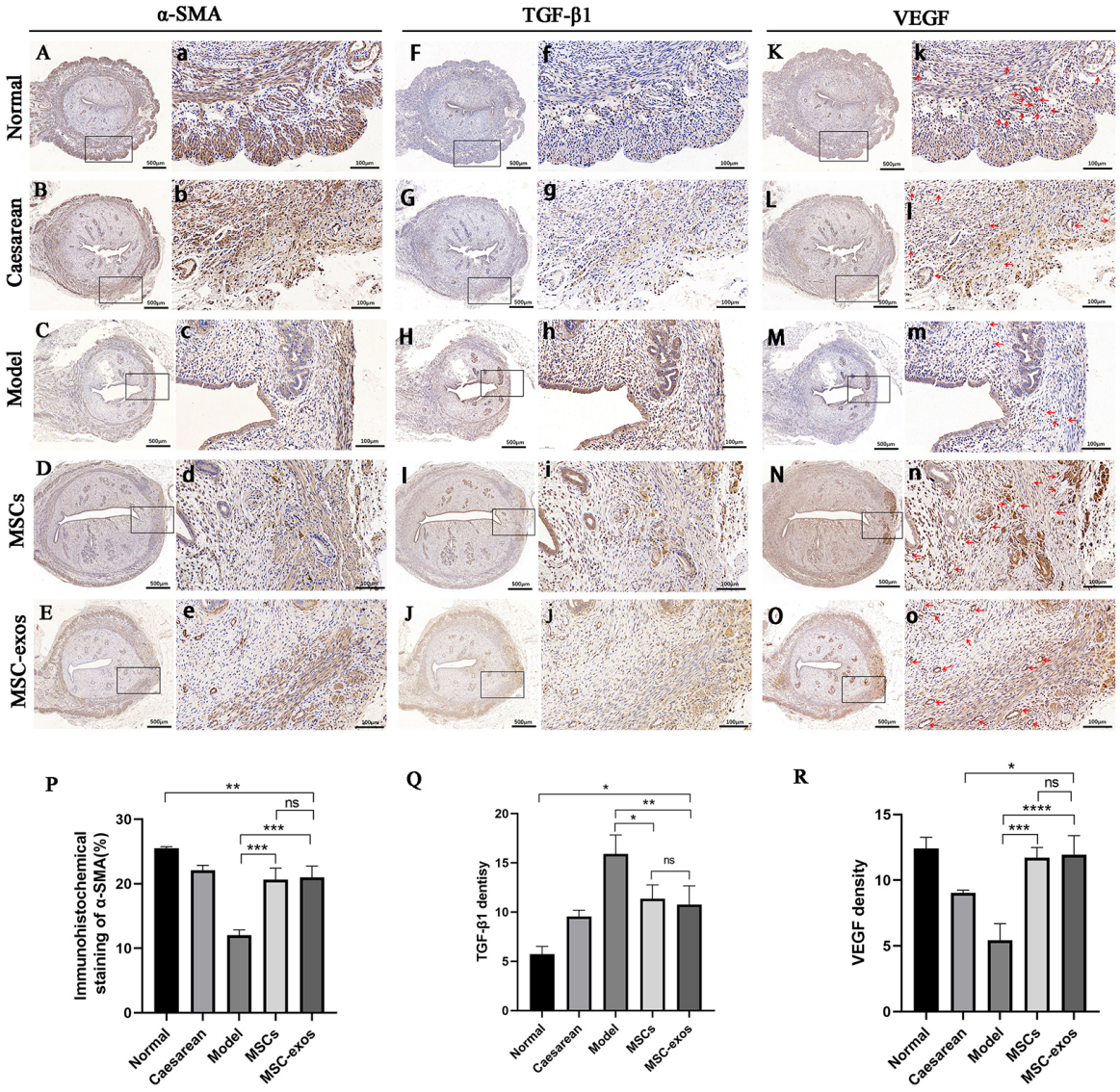

Fig. 5. Immunohistochemical assessment of a-SMA, TGF-β1, and VEGF protein expression 8 weeks after treatment with different methods. (A–E,a–e) α-SMA protein expression. (F–J,f–j) TGF-β1 protein expression. (K–O,k–o) VEGF protein expression. Red arrows indicate capillary density. (A–O) Scale bar = 500 µm; (a–o) Scale bar = 100 µm. (P) Statistical analysis of the percentage of positive area for α-SMA protein. (Q) Statistical analysis of TGF-β1 protein optical density values. (R) Statistical analysis of VEGF protein optical density values. *$p < 0.05$, **$p < 0.01$, ***$p < 0.001$, ****$p < 0.0001$, ns $p > 0.05$.

α-SMA and VEGF, thereby promoting regeneration of uterine smooth muscle and blood vessels.

hUCMSC-Exos Transplantation Promotes Restoration of Fertility in PCSD Rats

To evaluate the effects of different treatments on uterine function in rats with poorly healed uterine scars after caesarean delivery, we analyzed pregnancy rate, the number of implantations, fetal size and quality, and the ability to maintain pregnancy to late gestation in the operated uterine horns. All rats in the normal group became pregnant (100%), and the pregnancy rates in the caesarean, MSCs, and MSC-Exos groups were comparable (all 80%) and were substantially higher than in the model group (30%) (Table 1). Analysis of the implantation sites indicated that, in all post-surgical pregnancies, embryos are implanted within the scarred regions of the uterine horns (Fig. 7A–J).

As shown in Fig. 7K, the number of implanted embryos was significantly lower in the model group compared to the normal group (14.33 $\pm$ 1.90 vs 2.33$\pm$ 0.52, $p <$ 0.001). In contrast, MSC-Exos treatment significantly increased the number of implanted embryos compared to the model group (2.33 $\pm$ 0.52 vs 7.67 $\pm$ 0.52, $p < 0.01$). There were no statistical differences among the caesarean group, MSCs group, and MSC-Exos groups ($p > 0.05$).

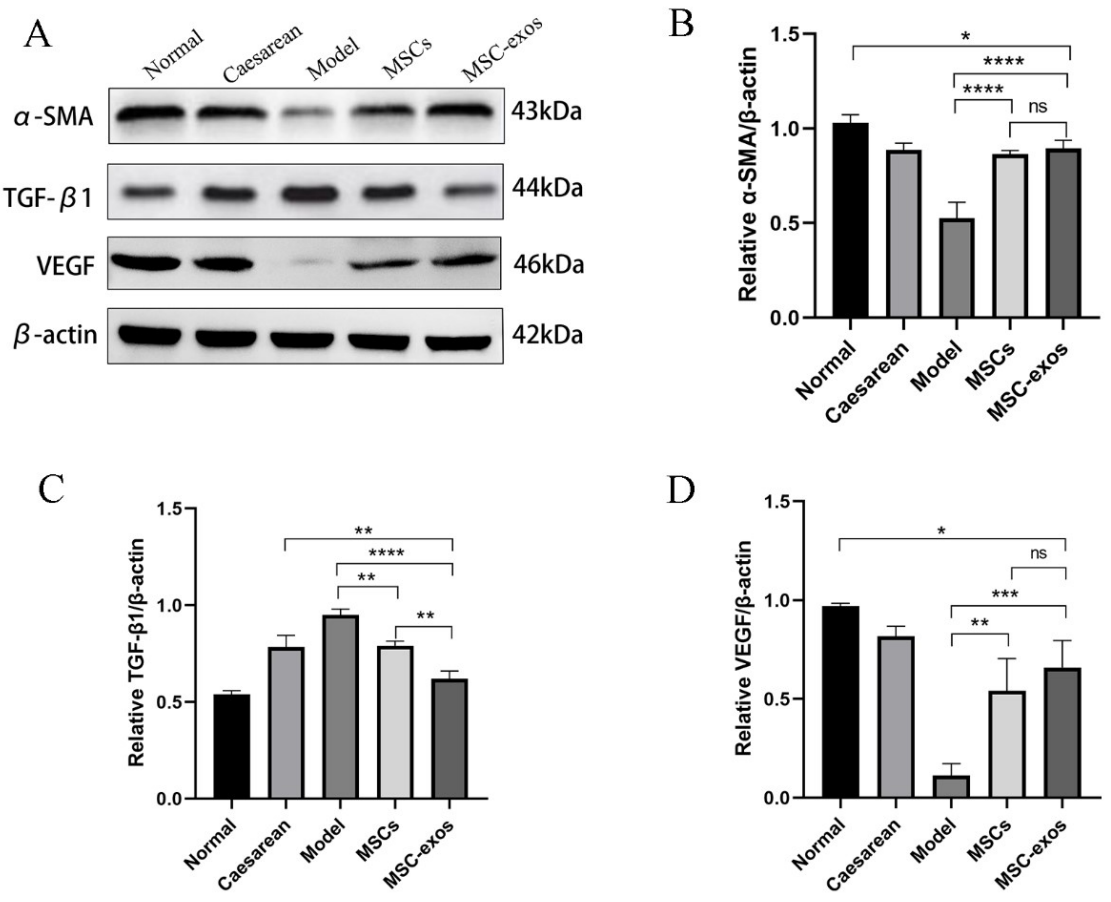

Fig. 6. Relative expression levels of α-SMA, TGF-β1, and VEGF proteins were detected using Western blot analysis at 8 weeks post-treatment with different methods. (A) The bands for α-SMA, TGF-β1, VEGF, and the β-actin (a housekeeping protein). Gray values were calculated for protein expression levels across groups to determine relative expression levels. (B) Relative expression of α-SMA protein. (C) Relative expression of TGF-β1 protein. (D) Relative expression of VEGF protein. *$p < 0.05$, **$p < 0.01$, ***$p < 0.001$, ****$p < 0.0001$, ns $p > 0.05$.

Table 1. Comparative reproductive outcomes of different treatment approaches.

Variable	Total number of uterine horns	Pregnant uterine horns (%)	Uterine horns with embryo in the scar area (%)
Normal group	8	8 (100%)	
Caesarean group	10	8 (80%)	8 (80%)
Model group	10	3 (30%)	3 (30%)
MSCs group	10	8 (80%)	8 (80%)
MSC-Exos group	10	8 (80%)	8 (80%)
p value		0.026	

MSCs, mesenchymal stem cells.

Further analysis of fetal size and quality revealed that some embryos in the model group were poorly developed, whereas fetal size and morphology were comparable among the other four groups (Fig. 7F–J). Furthermore, all groups were able to maintain pregnancy to late gestation without uterine rupture. These fertility outcomes demonstrate that both hUCMSCs and hUCMSC-Exos treatments effectively improve reproductive outcomes and restore fertility in rats with PCSD.

Discussion

The integrity of the endometrial basal layer is crucial for physiological endometrial repair, which involves coordinated interactions among various cell types, cytokines, and extracellular matrix components [28,29]. Uterine smooth muscle cells are relatively stable and have inherently limited regenerative capacity. Post-injury, reconnection of myocytes occurs slowly and is primarily mediated

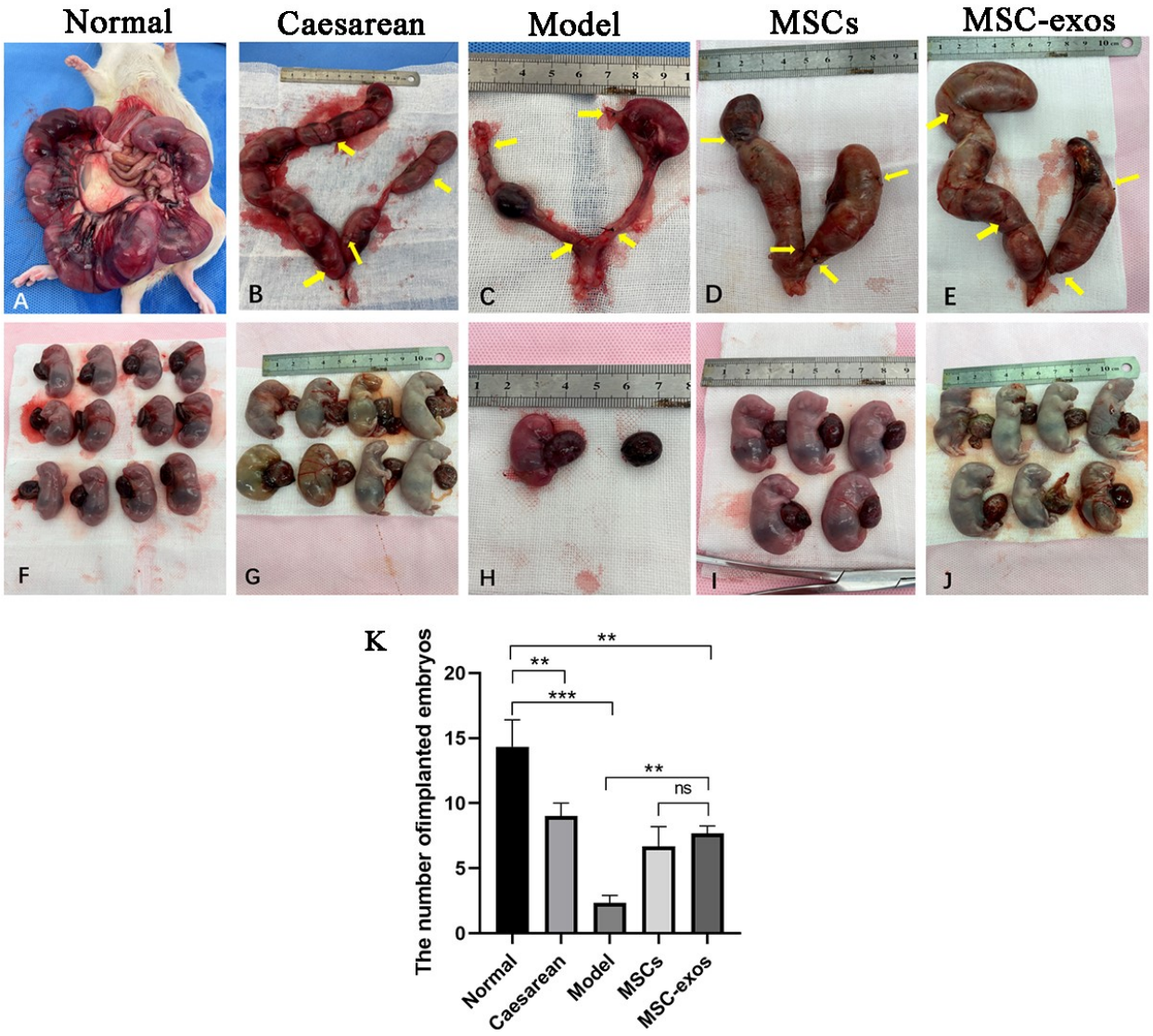

Fig. 7. Effects of different treatment methods on pregnancy outcomes in PCSD rats. (A–E) Appearance of uterine horns at term gestation in each group, with scar areas indicated between the two yellow arrows. (F–J) Number of term fetuses delivered in each group; (K) Statistical summary of fetal counts across groups. $^{**}p < 0.01$, $^{***}p < 0.001$, ns $p > 0.05$.

by fibrotic scar tissue at the rupture site [30]. Severe trauma from caesarean sections, curettage, or infection can deplete resident stem cells and myocytes, which triggers excessive fibroblast activation and persistent collagen secretion. This fibrotic response hinders the proliferation, differentiation, and migration of native uterine cells, ultimately resulting in collagenous scar formation at the damaged site [4]. Physiological scars resemble the surrounding tissue in texture with mild collagen deposition and usually do not cause dysfunction, requiring no intervention. In contrast, pathological scars are harder than normal tissue, characterized by excessive collagen deposition, which significantly impairs uterine function.

To investigate whether hUCMSC-Exos promote PCSD repair, establishing a reliable uterine injury model was essential. Previous studies have established a full-thickness uterine injury model by excising a 1.5 cm × 0.5 cm segment from each uterine horn while preserving the uterine mesentery [16,27,31]. However, these models are based on non-pregnant rats, in which the local uterine pathophysiology and healing processes may differ significantly from those in pregnant rats. Our study simulated common clinical causes of PCSD by inducing uterine injury during caesarean section through a combination of physical trauma and infection. Gross observations revealed hydrosalpinx in some rats, indicating intrauterine adhesions. H&E and Masson staining confirmed significant thinning of the uterine wall and proliferative fibrotic changes, supporting the successful development of a severe post-caesarean uterine injury model. Research on MSC-derived exosomes in

PCSD remains limited and has typically been restricted to non-pregnant models. To our knowledge, this study is the first to explore the therapeutic effects of hUCMSC-Exos in a pregnant rat model of PCSD.

Endometrial thickness and the degree of fibrosis are key predictors of uterine functional status and indicators of endometrial receptivity. In this study, H&E and Masson staining were used to assess histological recovery post-treatment. Our findings confirmed that both hUCMSC-Exos and hUCMSCs promoted endometrial growth and reduced fibrosis in PCSD rats. Myometrial thickness, smooth muscle cell density, and reduced fibrosis are closely associated with uterine contractile ability. Therefore, in addition to H&E and Masson staining, IHC and Western blot analysis were used to quantify α-SMA, TGF-β1 and VEGF expression. The findings showed that both hUCMSC-Exos and hUCMSCs treatment significantly downregulated TGF-β1, and upregulated α-SMA and VEGF levels after injury, which are crucial growth factors for uterine tissue regeneration [32,33]. These findings align with previous studies on MSC-based therapies for uterine tissue incision repair [16,27,31].

Reconstruction of a functional vascular network is a key determinant of successful wound repair. Angiogenesis plays a crucial role in tissue repair following injury, as newly formed blood vessels supply oxygen and nutrients to cells at the wound site, and inadequate local angiogenesis is considered a key contributor to impaired healing. VEGF is the most important growth factor regulating angiogenesis during tissue repair [34–36]. In the present study, we observed increased VEGF expression and enhanced neovascularization in the regenerating uterine horn of the hUCMSC-Exos treatment group. A study by Lin *et al*. [33] demonstrated a positive reparative role of collagen-binding VEGF in remodeling a scarred uterus. Braun *et al*. [37] found that mesenchymal stem cell-derived exosomes can support proangiogenic mechanisms by carrying VEGF, thereby improving pulmonary vascular growth in a model of neonatal bronchopulmonary dysplasia. These findings are consistent with our results.

Despite the well-established role of VEGF in enhancing angiogenesis, the specific mechanisms by which hUCMSC-Exos activate angiogenic pathways remain incompletely defined. While hUCMSC-Exos promote angiogenesis in injured uterine tissue and upregulate VEGF expression, it is not yet clear whether their proangiogenic effects are mediated directly through VEGF or via additional factors. Previous studies suggest that mesenchymal stem cell-derived exosomes promote angiogenesis is complex, likely involving multiple mechanisms, pathways, and factors [38–40]. Our future study will focus on elucidating the molecular mechanism through which hUCMSC-Exos drive angiogenesis to repair the injured uterus.

Restoration of fertility and ability to maintain pregnancy to full term is the gold standard for assessing the effectiveness of treatments for defective uterine scar healing, which most directly reflects functional recovery. To further verify the therapeutic effect of hUCMSC-Exos, male and female rats in each group were mated 8 weeks after treatment, and pregnancy outcomes were documented. In our study, pregnancy rates in the MSC-Exos and MSCs groups were significantly higher than in the model group, but remained lower than in the normal group, and were comparable to the caesarean group. This improvement may be related to the rapid improvement of endometrial tolerance after hUCMSC-Exos and hUCMSCs transplantation.

An interesting finding was that, in all pregnant rats, embryo implantation occurred within the scarred regions of the uterine horns. These findings differ from the results of Xu *et al*. [16], Zeng *et al*. [27], and Wang *et al*. [31], which may be related to differences in modeling approaches. In these studies, partial resection of the non-pregnant uterine wall was used to induce full-thickness uterine injury, whereas our model more appropriately reflects the clinical occurrence of post-caesarean section scar defect (PCSD), using a combination of infection and mechanical injury. This may further indicate the occurrence of scar pregnancy in our model. The mechanisms by which these scar pregnancies in rats could be maintained to full term without uterine rupture need to be further investigated.

Our findings also revealed that the number of fetuses in the MSC-Exos and MSCs groups was significantly higher than in the model group. The size of fetuses within the injured region was similar to that in the normal area. However, there were dysplastic fetuses in the damaged area in the model group. These observations suggest better embryo quality in the MSC-Exos and MSCs groups, indicating that the uterine vascular system may have been sufficiently repaired to support embryonic growth, and that the regenerated tissue could accommodate fetal development without uterine rupture. The slightly higher number of fetuses in the MSC-Exos group than in the MSCs group may be related to the low *in vivo* survival rate and partial apoptosis of directly transplanted MSCs.

Administration of hUCMSCs and hUCMSC-Exos in the rat PCSD model showed significant therapeutic effects. However, the data also indicate that outcomes in the hUCMSCs and hUCMSC-Exos treatment groups were not markedly superior compared to the standard caesarean section group across all parameters. We hypothesize that this result may be related to the excessive severity of injury in our model, which likely exceeds that observed in typical clinical PCSD. Consequently, the current interventions appear capable of restoring tissue structure and function to a level comparable with standard caesarean section, without yet achieving complete regeneration of the damaged tissue.

Furthermore, hUCMSC-Exos had therapeutic effects comparable to those of an equivalent dose of hUCMSCs. The route and nature of exosome administration may explain this finding. Transplanted hUCMSCs are living cells

that can continuously proliferate and maintain biological activity at the injury site. In contrast, hUCMSC-Exos are cellular components that cannot self-renew and may be gradually metabolized or cleared *in vivo*, thereby decreasing their sustained activity. Therefore, repeated transplantations might be necessary to achieve optimal therapeutic effects. For instance, Braun *et al*. [37] maintained a stable exosome therapeutic effect over a 14-day course in a rat lung injury model by administering hUCMSC-Exos intraperitoneally on a daily basis. Similarly, Zhang *et al*. [41] revealed that MenSCs-Exos injections at 4.5-day intervals were more effective in treating intrauterine adhesions than a single injection of the same total dose.

In our study, hUCMSCs and hUCMSC-Exos were injected directly into the injury site, thereby avoiding losses associated with homing after intravenous or intraperitoneal injection. Because PCSD rats might not tolerate repeated laparotomies over a short interval, we adopted a single local injection of hUCMSC-Exos. Improvement of exosome transplantation approaches will be a crucial focus of future investigation. Although the role of mesenchymal stem cells in promoting tissue regeneration is widely recognized, safety concerns such as tumorigenicity and embolism risk remain. Their derived exosomes possess comparable regenerative effects while offering benefits including nanoscale size, high biocompatibility, stability in body fluids, a favorable safety profile, and a lack of genetic information. These characteristics make hUCMSC-Exos a promising candidate for managing uterine tissue injury, including PCSD.

Our study has several limitations. First, the fertility evaluation did not include observing or comparing the delivery process, and it remains unknown whether the repaired uterus can tolerate the mechanical stress of labor. Second, the optimal dose and delivery method of hUCMSC-Exos have not yet been defined, and further exploration is warranted to achieve tissue repair that more closely approximates normal uterine structure. Third, the mechanisms by which hUCMSC-Exos enhance PCSD repair are not fully elucidated, necessitating further research to identify the molecular mechanisms to clarify how these exosomes promote regeneration of the damaged uterine wall.

In summary, our findings demonstrate that both hUCMSCs and hUCMSC-Exos promote uterine regeneration and repair and improve fertility in PCSD model rats. hUCMSC-Exos appear to offer certain advantages over hUCMSCs, including stronger upregulation of angiogenesis-related proteins like VEGF and improved number and quality of embryos after mating. These findings indicate that hUCMSC-Exos represent a promising and robust therapeutic approach for improving PCSD treatment.

Conclusion

This study reveals that hUCMSC-Exos demonstrate promising therapeutic efficacy in the PCSD model. Transplantation of hUCMSC-Exos promotes regeneration of the endometrium, myometrium, and vasculature within the uterine scar, while also improving fertility outcomes. These observations suggest that transplantation of hUCMSC-Exos may represent a highly promising cell-free therapeutic option for patients with PCSD.

Availability of Data and Materials

The datasets used and/or analyzed during the current study are available from the corresponding authors upon reasonable request.

Author Contributions

JJ, LY and LC conceived and designed the experiments, and wrote the article; JJ and QP performed the experiments, analyzed and interpreted the data; YH and SY provided reagents and materials and contributed to data analysis; DL conducted literature search, analyzed data and translated the manuscript. All authors contributed to critical revision of the manuscript for important intellectual content. All authors have read and approved the final manuscript. All authors have participated sufficiently in the work and agreed to be accountable for all aspects of the work.

Ethics Approval and Consent to Participate

The experimental protocol was approved by the Animal Care Welfare Committee of Guizhou Medical University (Approval number: 2304384).

Acknowledgment

Not applicable.

Funding

This study was supported by the Science and Technology Foundation of Guizhou Provincial Health Commission (gzwkj2021–081).

Conflict of Interest

The authors declare no conflict of interest.

References

[1] Di Spiezio Sardo A, Saccone G, McCurdy R, Bujold E, Bifulco G, Berghella V. Risk of Cesarean scar defect following single- vs double-layer uterine closure: systematic review and meta-analysis of randomized controlled trials. Ultrasound in Obstetrics & Gynecology: the Official Journal of the International

Society of Ultrasound in Obstetrics and Gynecology. 2017; 50: 578–583. https://doi.org/10.1002/uog.17401.

[2] Vervoort AJMW, Uittenbogaard LB, Hehenkamp WJK, Brölmann HAM, Mol BWJ, Huirne JAF. Why do niches develop in Caesarean uterine scars? Hypotheses on the aetiology of niche development. Human Reproduction (Oxford, England). 2015; 30: 2695–2702. https://doi.org/10.1093/humrep/dev240.

[3] Higuchi A, Tsuji S, Nobuta Y, Nakamura A, Katsura D, Amano T, *et al*. Histopathological evaluation of cesarean scar defect in women with cesarean scar syndrome. Reproductive Medicine and Biology. 2021; 21: e12431. https://doi.org/10.1002/rmb2.12431.

[4] Glenn TL, Han E. Cesarean scar defect: far from understood. Fertility and Sterility. 2021; 116: 369–370. https://doi.org/10.1016/j.fertnstert.2021.06.006.

[5] Siraj SHM, Lional KM, Tan KH, Wright A. Repair of the myometrial scar defect at repeat caesarean section: a modified surgical technique. BMC Pregnancy and Childbirth. 2021; 21: 559. https://doi.org/10.1186/s12884-021-04040-9.

[6] Tsuji S, Nobuta Y, Hanada T, Takebayashi A, Inatomi A, Takahashi A, *et al*. Prevalence, definition, and etiology of cesarean scar defect and treatment of cesarean scar disorder: A narrative review. Reproductive Medicine and Biology. 2023; 22: e12532. https://doi.org/10.1002/rmb2.12532.

[7] Lin PL, Hou JH, Chen CH. A common problem between gynecology, obstetrics, and reproductive medicine: Cesarean section scar defect. Taiwanese Journal of Obstetrics & Gynecology. 2024; 63: 459–470. https://doi.org/10.1016/j.tjog.2024.03.018.

[8] Bernard C, Agostini A, Bretelle F, Blanc J, Netter A. Risk factors and influence of surgical technique on the risk of caesarean scar defect formation: A systematic review of the literature. Journal of Gynecology Obstetrics and Human Reproduction. 2025; 54: 102870. https://doi.org/10.1016/j.jogoh.2024.102870.

[9] Antila-Långsjö RM, Mäenpää JU, Huhtala HS, Tomás EI, Staff SM. Cesarean scar defect: a prospective study on risk factors. American Journal of Obstetrics and Gynecology. 2018; 219: 458.e1–458.e8. https://doi.org/10.1016/j.ajog.2018.09.004.

[10] van der Voet LF, Vervoort AJ, Veersema S, BijdeVaate AJ, Brölmann HA, Huirne JA. Minimally invasive therapy for gynaecological symptoms related to a niche in the caesarean scar: a systematic review. BJOG : an international journal of obstetrics and gynaecology. 2014; 121: 145–156. https://doi.org/10.1111/1471-0528.12537.

[11] Tower AM, Frishman GN. Cesarean scar defects: an underrecognized cause of abnormal uterine bleeding and other gynecologic complications. Journal of Minimally Invasive Gynecology. 2013; 20: 562–572. https://doi.org/10.1016/j.jmig.2013.03.008.

[12] Donnez O. Cesarean scar defects: management of an iatrogenic pathology whose prevalence has dramatically increased. Fertility and Sterility. 2020; 113: 704–716. https://doi.org/10.1016/j.fertnstert.2020.01.037.

[13] Dominguez JA, Pacheco LA, Moratalla E, Carugno JA, Carrera M, Perez-Milan F, *et al*. Diagnosis and management of isthmocele (Cesarean scar defect): a SWOT analysis. Ultrasound in Obstetrics & Gynecology: the Official Journal of the International Society of Ultrasound in Obstetrics and Gynecology. 2023; 62: 336–344. https://doi.org/10.1002/uog.26171.

[14] Rodríguez-Eguren A, Gómez-Álvarez M, Francés-Herrero E, Romeu M, Ferrero H, Seli E, *et al*. Human Umbilical Cord-Based Therapeutics: Stem Cells and Blood Derivatives for Female Reproductive Medicine. International Journal of Molecular Sciences. 2022; 23: 15942. https://doi.org/10.3390/ijms232415942.

[15] Hoang DM, Pham PT, Bach TQ, Ngo ATL, Nguyen QT, Phan TTK, *et al*. Stem cell-based therapy for human diseases. Signal Transduction and Targeted Therapy. 2022; 7: 272. https://doi.org/10.1038/s41392-022-01134-4.

[16] Xu L, Ding L, Wang L, Cao Y, Zhu H, Lu J, *et al*. Umbilical cord-derived mesenchymal stem cells on scaffolds facilitate collagen degradation via upregulation of MMP-9 in rat uterine scars. Stem Cell Research & Therapy. 2017; 8: 84. https://doi.org/10.1186/s13287-017-0535-0.

[17] Kim HJ, Park JS. Usage of Human Mesenchymal Stem Cells in Cell-based Therapy: Advantages and Disadvantages. Development & Reproduction. 2017; 21: 1–10. https://doi.org/10.12717/DR.2017.21.1.001.

[18] Deng H, Sun C, Sun Y, Li H, Yang L, Wu D, *et al*. Lipid, Protein, and MicroRNA Composition Within Mesenchymal Stem Cell-Derived Exosomes. Cellular Reprogramming. 2018; 20: 178–186. https://doi.org/10.1089/cell.2017.0047.

[19] Hade MD, Suire CN, Suo Z. Mesenchymal Stem Cell-Derived Exosomes: Applications in Regenerative Medicine. Cells. 2021; 10: 1959. https://doi.org/10.3390/cells10081959.

[20] Tan F, Li X, Wang Z, Li J, Shahzad K, Zheng J. Clinical applications of stem cell-derived exosomes. Signal Transduction and Targeted Therapy. 2024; 9: 17. https://doi.org/10.1038/s41392-023-01704-0.

[21] El-Din SS, Aboulhoda BE, Hassouna A, Shakweer MM, Alghamdi MA, Essam D, *et al*. The Role of Intra-Articular Delivery of BM-MSCs-Derived Exosomes in Improving Osteoarthritis: Implication of circYAP1/miRNA-21/TLR7 Axis. Discovery Medicine. 2024; 36: 1420–1429. https://doi.org/10.24976/Discov.Med.202436186.132.

[22] Su W, Yin Y, Zhao J, Hu R, Zhang H, Hu J, *et al*. Exosomes derived from umbilical cord-derived mesenchymal stem cells exposed to diabetic microenvironment enhance M2 macrophage polarization and protect against diabetic nephropathy. FASEB journal : official publication of the Federation of American Societies for Experimental Biology. 2024; 38: e23798. https://doi.org/10.1096/fj.202400359R.

[23] Zhang WY, Wen L, Du L, Liu TT, Sun Y, Chen YZ, *et al*. S-RBD-modified and miR-486-5p-engineered exosomes derived from mesenchymal stem cells suppress ferroptosis and alleviate radiation-induced lung injury and long-term pulmonary fibrosis. Journal of Nanobiotechnology. 2024; 22: 662. https://doi.org/10.1186/s12951-024-02830-9.

[24] Xie Y, Sun Y, Liu Y, Zhao J, Liu Q, Xu J, *et al*. Targeted Delivery of RGD-CD146+CD271+ Human Umbilical Cord Mesenchymal Stem Cell-Derived Exosomes Promotes Blood-Spinal Cord Barrier Repair after Spinal Cord Injury. ACS Nano. 2023; 17: 18008–18024. https://doi.org/10.1021/acsnano.3c04423.

[25] Zhang X, Ma L, Liu X, Zhou X, Wang A, Lai Y, *et al*. Sustained release of miR-21 carried by mesenchymal stem cell-derived exosomes from GelMA microspheres inhibits ovarian granulosa cell apoptosis in premature ovarian insufficiency. Mater Today Bio. 2025; 31: 101469. https://doi.org/10.1016/j.mtbio.2025.101469.

[26] Li X, Duan H, Wang S, Lv CX. Umbilical cord mesenchymal stem cell-derived exosomes reverse endometrial fibrosis by the miR-145-5p/ZEB2 axis in intrauterine adhesions. Reproductive Biomedicine Online. 2023; 46: 234–243. https://doi.org/10.1016/j.rbmo.2022.05.018.

[27] Zeng X, Liao Y, Huang D, Yang J, Dai Z, Chen Z, *et al*. Exosomes derived from hUC-MSCs exhibit ameliorative efficacy upon previous cesarean scar defect via orchestrating β-TrCP/CHK1 axis. Scientific Reports. 2025; 15: 489. https://doi.org/10.1038/s41598-024-84689-2.

[28] Zhao LM, Da LC, Wang R, Wang L, Jiang YL, Zhang XZ, *et al*. Promotion of uterine reconstruction by a tissue-engineered uterus with biomimetic structure and extracellular matrix microenvironment. Science Advances. 2023; 9: eadi6488. https://doi.org/10.1126/sciadv.adi6488.

[29] Maybin JA, Critchley HOD. Menstrual physiology: implications for endometrial pathology and beyond. Human Reproduction Update. 2015; 21: 748–761. https://doi.org/10.1093/humupd/dmv038.

[30] Wu C, Chen X, Mei Z, Zhou J, Wu L, Chiu WH, *et al*. A preliminary study of uterine scar tissue following cesarean section. Journal of Perinatal Medicine. 2018; 46: 379–386. https://doi.org/10.1515/jpm-2016-0347.

[31] Wang H, Yang X, Chen X, Xie H, Wang J, Zhang Y. Identify the role of Human Wharton's Jelly Mesenchymal Stem Cells in repairing injured uterine of rat. The Journal of Obstetrics and Gynaecology Research. 2021; 47: 320–328. https://doi.org/10.1111/jog.14526.

[32] Ding L, Li X, Sun H, Su J, Lin N, Péault B, *et al*. Transplantation of bone marrow mesenchymal stem cells on collagen scaffolds for the functional regeneration of injured rat uterus. Biomaterials. 2014; 35: 4888–4900. https://doi.org/10.1016/j.biomaterials.2014.02.046.

[33] Lin N, Li X, Song T, Wang J, Meng K, Yang J, *et al*. The effect of collagen-binding vascular endothelial growth factor on the remodeling of scarred rat uterus following full-thickness injury. Biomaterials. 2012; 33: 1801–1807. https://doi.org/10.1016/j.biomaterials.2011.11.038.

[34] Eming SA, Martin P, Tomic-Canic M. Wound repair and regeneration: mechanisms, signaling, and translation. Science Translational Medicine. 2014; 6: 265sr6. https://doi.org/10.1126/scitranslmed.3009337.

[35] Novosel EC, Kleinhans C, Kluger PJ. Vascularization is the key challenge in tissue engineering. Advanced Drug Delivery Reviews. 2011; 63: 300–311. https://doi.org/10.1016/j.addr.2011.03.004.

[36] Fan Y, Sun J, Zhang Q, Lai D. Transplantation of human amniotic epithelial cells promotes morphological and functional regeneration in a rat uterine scar model. Stem Cell Research & Therapy. 2021; 12: 207. https://doi.org/10.1186/s13287-021-02260-6.

[37] Braun RK, Chetty C, Balasubramaniam V, Centanni R, Haraldsdottir K, Hematti P, *et al*. Intraperitoneal injection of MSC-derived exosomes prevent experimental bronchopulmonary dysplasia. Biochemical and Biophysical Research Communications. 2018; 503: 2653–2658. https://doi.org/10.1016/j.bbrc.2018.08.019.

[38] Zhang B, Wu X, Zhang X, Sun Y, Yan Y, Shi H, *et al*. Human umbilical cord mesenchymal stem cell exosomes enhance angiogenesis through the Wnt4/β-catenin pathway. Stem Cells Translational Medicine. 2015; 4: 513–522. https://doi.org/10.5966/sctm.2014-0267.

[39] Qu Q, Liu L, Wang L, Cui Y, Liu C, Jing X, *et al*. Exosomes derived from hypoxic mesenchymal stem cells restore ovarian function by enhancing angiogenesis. Stem Cell Research & Therapy. 2024; 15: 496. https://doi.org/10.1186/s13287-024-04111-6.

[40] Zhang L, Ouyang P, He G, Wang X, Song D, Yang Y, *et al*. Exosomes from microRNA-126 overexpressing mesenchymal stem cells promote angiogenesis by targeting the PIK3R2-mediated PI3K/Akt signalling pathway. Journal of Cellular and Molecular Medicine. 2021; 25: 2148–2162. https://doi.org/10.1111/jcmm.16192.

[41] Zhang S, Chang Q, Li P, Tong X, Feng Y, Hao X, *et al*. Concentrated small extracellular vesicles from menstrual blood-derived stromal cells improve intrauterine adhesion, a pre-clinical study in a rat model. Nanoscale. 2021; 13: 7334–7347. https://doi.org/10.1039/d0nr08942g.